

Article

# Composition, Sources, and Distribution of PM<sub>2.5</sub> Saccharides in a Coastal Urban Site of China

Mengxin Xiao <sup>1</sup>, Qiongzhen Wang <sup>2</sup>, Xiaofei Qin <sup>1</sup>, Guangyuan Yu <sup>1</sup> and Congrui Deng <sup>1,\*</sup>

<sup>1</sup> Shanghai Key Laboratory of Atmospheric Particle Pollution and Prevention (LAP3), Department of Environmental Science and Engineering, Fudan University, Shanghai 200433, China; 15210740018@fudan.edu.cn (M.X.); 17110740018@fudan.edu.cn (X.Q.); 16210740016@fudan.edu.cn (G.Y.)

<sup>2</sup> Environmental Science Research and Design Institute of Zhejiang Province, Hangzhou 310007, China; wangqz03@126.com

\* Correspondence: dcr.0807@163.com; Tel.: +86-137-6468-1187

Received: 2 June 2018; Accepted: 16 July 2018; Published: 17 July 2018



**Abstract:** The characteristics of biogenic aerosols in an urban area were explored by determining the composition and temporal distribution of saccharides in PM<sub>2.5</sub> in Shanghai. The total saccharides showed a wide range of 9.4 ng/m<sup>3</sup> to 1652.9 ng/m<sup>3</sup>, with the averaged concentrations of 133.1 ng/m<sup>3</sup>, 267.5 ng/m<sup>3</sup>, 265.1 ng/m<sup>3</sup>, and 674.4 ng/m<sup>3</sup> in spring, summer, autumn, and winter, respectively. The saccharides include anhydrosaccharides (levoglucosan and mannosan), which were higher in cold seasons due to the increased biomass burning; saccharide alcohols (mannitol, arabitol, sorbitol); and monosaccharides (fructose, glucose), which were more abundant in warm seasons and attributed to the biological emissions. Through positive matrix factorization (PMF) analysis, four emission sources of saccharides were resolved, including biomass burning, fungal spores, plant decomposition, and pollen. Moreover, the process analysis of high concentrations of levoglucosan was conducted by backward trajectory and fire points. We found that concentrations of anhydrosaccharides were relatively stable under different pollution levels, while saccharide alcohols exhibited an obvious decrease with the concentration of PM<sub>2.5</sub>, indicating that biomass burning was not the core reason for heavy haze pollution. However, high level PM<sub>2.5</sub> pollution might inhibit the effects of biological activities.

**Keywords:** saccharides; biomass burning; haze; source apportionment; bio-aerosol

## 1. Introduction

Organic aerosols are important parts of fine atmospheric particulate matter, which account for about 20–60% of the PM<sub>2.5</sub> mass in urban sites, 30–50% in remote areas, and even up to 90% in the low troposphere [1]. The composition of organic aerosols is very complex and diverse with variable characteristics, among which the water-soluble organic components (WSOC) are the most important species, and the percentage of WSOC in organic aerosols can reach as high as 80% [2,3]. WSOC in the atmosphere have attracted increased attention for their important roles in haze pollution and new particle formation due to their specific physical and chemical properties [4,5].

Saccharides are important substances of WSOC in aerosols, which account for 13–26% of the mass of continental aerosols, and 63% of the mass of marine aerosols [6]. Atmospheric saccharides mainly contain three species: Anhydrosaccharides, primary saccharides (monosaccharides and disaccharides), and saccharide alcohols. Anhydrosaccharides mainly include levoglucosan, mannosan, and galactosan, which originate from primary emissions during the process of biomass burning, and levoglucosan has been widely used as an effective tracer for biomass burning emissions [7].

Primary saccharides usually include monosaccharides (glucose, fructose) and disaccharides (sucrose, trehalose), which commonly exist in primary biological aerosol particles (PBAPs) that are emitted from microorganisms, fungal spores, pollen, biological crusts, lichens, and other like plant or animal fragments [8]. Fructose and glucose, from the degradation of the soil microorganisms, can also re-suspend together with soil dust by wind or some agricultural activities, therefore, fructose and glucose are proposed as tracers for soil suspension [9]. Saccharide alcohols, including mannitol, arabitol, and sorbitol, mainly originate from fungal spores, especially for mannitol and arabitol, which could account for more than 50% of the dry weight of fungal mycelium. Thus, saccharide alcohols could be used as tracers for fungal spores [10].

Biomass burning is a common source of air pollution [11–14]. Levoglucosan in ambient air is usually high in cold seasons due to heating demands. Bond et al. reported that about 60% of the primary pyrogenic organic carbon (OC) was a result of wood combustion in Europe [15], and the contribution of biomass burning emissions to OC was  $45\% \pm 12\%$  during the rice-harvest period in Korea [13]. In contrast, saccharides from biological sources showed the highest level in April (the spring bloom season) on Jeju Island, and sucrose contributed to as high as 80% of the total saccharides [16]. Primary saccharides (sucrose, fructose, glucose) showed a unimodal distribution, with a dominant peak occurring in coarse-particles, while anhydrosaccharides were more likely to exist in fine particles [17]. Until now, studies on saccharides have mainly been focused on levoglucosan to evaluate the contribution of biomass burning on air pollution, but information related to the other saccharides, especially those from biological derivations, is still limited, and the characteristics of saccharides during periods of variable pollution levels are lacking. However, with the substantial reduction of pollutants emitted from industrial processes, the contribution of natural sources and agricultural emissions to the atmosphere, especially PBAPs, has increasingly emerged and been highlighted as an area of interest [18–20].

Based on the determination of the chemical species in the  $PM_{2.5}$  of Shanghai, this study provides detailed information on the saccharides in atmospheric particle matters in urban areas, and demonstrates their seasonal distributions, emission sources, and the affected factors, especially for those from biological sources. The characteristics of saccharides are also discussed under different levels of fine particulate pollution.

## 2. Experiments

### 2.1. Sampling

The sampling site ( $31.3^\circ$  N,  $121.49^\circ$  E) in this study was on the roof (20 m) of the No.4 teaching building on the campus of Fudan University in the Yangpu District of Shanghai (Figure 1). It is considered as a representative urban site due to the mixed anthropogenic emission sources of industries, vehicle transportation, biomass burning, and so on [21]. The predominant wind directions in summer and winter are southeasterly and northwesterly, which is influenced by the Asian Monsoon [22].

The sampling period was between 18 March 2013 to 22 January 2014, and the periods of 18 March–26 April, 16 July–17 August, 29 October–29 November, and 30 November–22 January 2014 represent spring, summer, autumn, and winter, respectively.  $PM_{2.5}$  samples were collected on Quartz filters under a medium flow rate of 100 L/min with a  $PM_{2.5}$  sampler (HY-100c, Qingdao Hengyuan, China), where the duration time for each sample was usually 23.5 h.

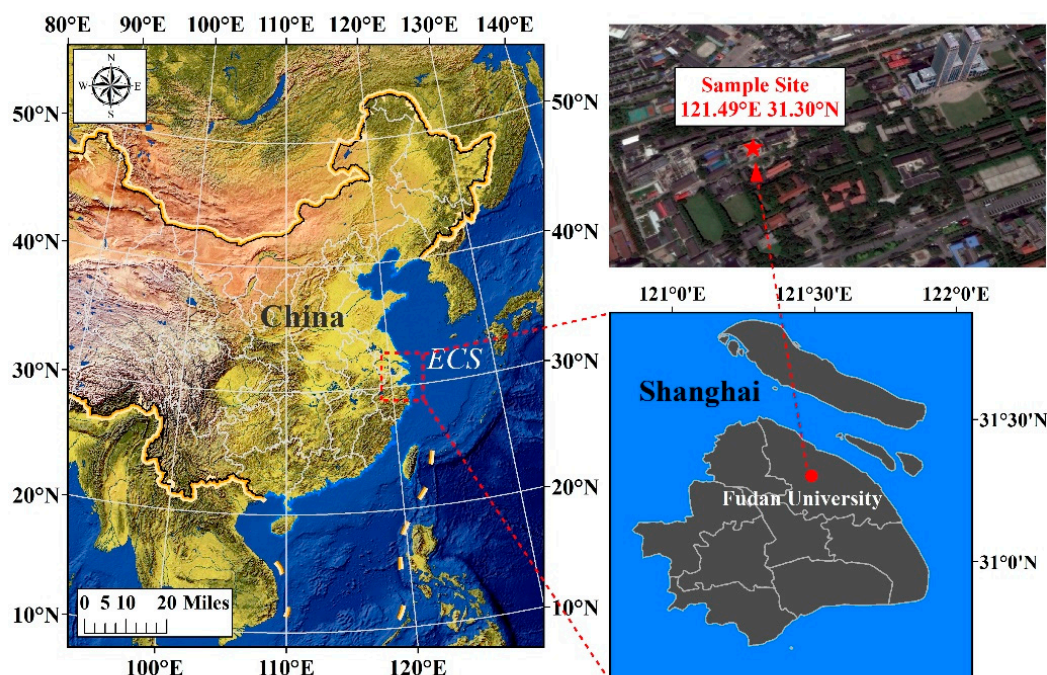


**Figure 1.** The location of the sampling site (marked with a red five-pointed star).

## 2.2. Chemical Analysis

A quarter of the sampled quartz filter was shredded and ultrasonically extracted three times with 20 mL dichloromethane/methanol (*v/v*, 1:1), and the extracting solution was combined together before a mixture of methyl- $\beta$ -D-xylanopyranoside (MXP) and cis-ketopinic acid (KPA) was added as the internal/recovery standard. After being concentrated to about 1 mL with a rotary evaporator (IKA, RV10, Staufen, Germany), the samples were filtered through quartz wool in glass droppers, and the filtrate was blown to near dry using a nitrogen blowing instrument (Anpel, DC-12-RT, Shanghai, China). The derivatization reaction was then carried out by adding 100  $\mu$ L N, O-bis-(trimethylsilyl)-trifluoroacetamide (BSTFA, with 1% trimethylchlorosilane as a catalyst) and 20 mL anhydrous pyridine at 75 °C for 45 min using a dry bath (MIU, DTH-100, Hangzhou, China). The reaction products were determined with a gas chromatography mass spectrometry (GC-MS) (Agilent, 7890 GC/5975 MSD, Santa Clara, CA, USA), equipped with a DB-5MS capillary column (30 m  $\times$  0.25 m  $\times$  0.25  $\mu$ m), and hexamethylbenzene was added as the internal standard. The temperature programming was initially set at 60 °C for 2 min, then increased to 300 °C at a rate of 5 °C min<sup>-1</sup> and held for 10 min. The MS was operated in EI mode at 70 eV, with a scan range of 50–550 amu. The temperature of the injection port was 290 °C, and the inlet quantity was 1  $\mu$ L. The detailed procedure is available in [23].

The chemicals in this study include: Dichloromethane (HPLC grade, CNW), methanol (HPLC grade, CNW), and hexane (HPLC grade, 95%, CNW); Levoglucosan (>99%), Mannosan (>98%), D(-)- Fructose (>99%),  $\alpha$ -D(+)- Grutose (>99%), D(+)- Arabitol (>99%), D(-)- Mannitol (99%), and D(-)- Sorbitol (>98%); BSTFA (>99%) and TMCS, anhydrous pyridine (99.5%, moisture content less than 0.005%, molecular sieve).

## 2.3. QA/QC

Before sampling, the quartz filters were wrapped in aluminum foil and then prebaked at 550 °C in a muffle furnace for 4 h. All empty and sampled filters were placed within plastic bags and stored at -20 °C in a refrigerator before sampling or being analyzed. After being flushed with chromic acid lotion, tap water, and deionized water successively, all glass vessels were dried at 120 °C for 5 h, then

baked at 450 °C for 4 h. To ensure the veracity of the experiments, field blanks were collected for each season with the same sampling operation procedure, but without the pump on, and the blanks were treated similarly to the sample filter to also conduct the solvent and instrument blank. To ensure the stable operation of the instrument, one standard sample was injected after 20 samples.

#### 2.4. Multiple Statistical Analysis

##### 2.4.1. Backward Trajectory Analysis

To better evaluate the contributions of air masses from different origins on saccharides in Shanghai, 48 h backward trajectory analyses with fire spots were performed from the sampling site at a height of 500 m a.s.l. by using a HYSPLIT (Hybrid Single Particle Lagrangian Integrated Trajectory) model. Burning activities were illustrated by fire spots, and the datasets were downloaded from MODIS Global Fire Mapping by Fire Information for Resource Management System (FIRMS).

##### 2.4.2. Potential Source Contribution Function (PSCF) Analysis

Potential source contribution function was calculated to infer the potential sources of the elevated concentrations of components at the receptor site [24]. The region covered by trajectories was divided into many grid cells of  $0.2^\circ \times 0.2^\circ$  and endpoints. Therefore, the PSCF value can be defined as:

$$PSCF_{ij} = m_{ij} / n_{ij} \quad (1)$$

where  $n_{ij}$  is the total trajectory numbers that fall in the grid cell ( $i, j$ ); and  $m_{ij}$  is the number of the endpoints with measured concentrations higher than the pollution criterion [25].

A higher value of PSCF implies a larger contribution of the region to the sampling site. However, since PSCF is a conditional probability, a low value of  $n_{ij}$  brings more uncertainty to the PSCF calculation results. To reduce the uncertainty, the weight function,  $W_{ij}$ , was introduced [26–29]:

$$WPSCF = W_{ij} \times PSCF \quad (2)$$

The weighting function reduced the PSCF values when the total number of the endpoints in a particular cell was less than about three times the average value of the end points per cell [28].

##### 2.4.3. Positive Matrix Factorization (PMF) Analysis

The US EPA PMF 5.0 model was used in our study, and the principle and operational approaches could be found online in the EPA 5.0 Fundamentals and User Guide. A matrix of sample data,  $x$ , was decomposed into a source contribution matrix,  $g$ , and a source strength matrix,  $f$  [30], where  $i$  and  $j$  were used to describe the number of samples and components species, and  $p$  is the number of source factors. Therefore,  $x_{ij}$  is the concentration of each species in each sample;  $g_{ik}$  is the contribution of each source to each sample;  $f_{ik}$  is the mass fraction of each species in each source; and  $e_{ij}$  is the residual for each sample.

The equation is shown in (3):

$$x_{ij} = \sum_{k=1}^p g_{ik} f_{kj} + e_{ij} \quad (3)$$

The results were constrained as no negative contribution from a source to a sample, therefore, the uncertainty caused by rotating factors was minimized. Moreover, the missing value was replaced by the median of the dataset, which is accompanied by a large uncertainty as well. The PMF solution minimizes the function,  $Q$ , based on the uncertainties ( $u$ ) as shown in (4) [31]:

$$Q = \sum_{i=1}^n \sum_{j=1}^m \left( \frac{e_{ij}}{u_{ij}} \right)^2 \quad (4)$$

### 3. Results and Discussion

#### 3.1. Concentrations and Seasonal Variations of Saccharides

Seven saccharides were detected during the sampling period, including two species of anhydrosaccharides (levoglucosan and mannosan), two species of monosaccharides (fructose and glucose), and three species of saccharide alcohols (mannitol, arabitol, and sorbitol).

Table 1 presents the concentrations of the seven saccharides in the PM<sub>2.5</sub> samples obtained in Shanghai during 2013. The total saccharides showed significant fluctuation, with daily concentrations ranging from 9.4 ng/m<sup>3</sup> to 1652.9 ng/m<sup>3</sup>. The annual average concentration of the total saccharides (346.9 ng/m<sup>3</sup>) in Shanghai was lower than those in Beijing (600 ng/m<sup>3</sup>) and Rajim (10,166 ng/m<sup>3</sup>) (Table 2). However, the levels of total saccharides in Shanghai were still higher than some sites, such as an urban site (6.2 ng/m<sup>3</sup>) and a rural site (38.8 ng/m<sup>3</sup>) in the Po Valley in Northern Italy (Table 2). Total saccharides showed obvious seasonal variation, where the average concentrations were 33.1 ng/m<sup>3</sup>, 267.5 ng/m<sup>3</sup>, 265.1 ng/m<sup>3</sup>, and 674.4 ng/m<sup>3</sup> in spring, summer, autumn, and winter, respectively.

**Table 1.** Seasonal mean concentrations of measured saccharides (ng/m<sup>3</sup>) in PM<sub>2.5</sub> samples in Shanghai.

Components	Spring		Summer		Autumn		Winter	
	Range	Average	Range	Average	Range	Average	Range	Average
levoglucosan	5.3–142.7	66.0	2.4–195.9	46.5	8.3–823.6	165.7	66.0–1064.1	392.2
mannosan	1.1–29.1	13.4	0.5–40.8	9.7	0.7–210.2	26.9	21.3–343.3	126.5
Total burning	6.4–171.8	79.4	2.9–236.8	56.2	6.9–858.0	192.6	87.3–1407.4	518.7
fructose	3.4–36.1	19.2	1.2–189.9	35.5	7.9–194.4	37.3	4.1–144.9	36.3
glucose	2.0–13.0	6.9	0.6–56.1	14.9	1.4–41.6	9.4	1.8–31.2	12.7
arabitol	0.8–17.6	5.4	0.4–58.9	14.9	1.1–46.2	8.7	1.7–33.4	7.3
mannitol	3.0–88.1	25.3	4.2–706.5	172.7	3.8–64.6	24.7	5.8–96.6	36.8
sorbitol	n.d.	n.d.	0.1–15.1	2.7	0.3–6.3	2.5	1.3–241.4	72.1
Total biological	7.8–153.9	53.7	6.5–1026.5	211.4	14.6–240.7	78.2	4.0–421.5	165.2
Total saccharides	23.7–310.3	133.1	9.4–1263.3	267.5	23.6–982.1	265.1	116.8–1652.9	674.4
PM <sub>2.5</sub>	46.5–287.3	94.5	22.6–205.3	62.8	68.2–208.0	120.8	56.9–416.5	155.9
TS/PM <sub>2.5</sub>	0.04–0.3%	0.1%	0.03–0.8%	0.3%	0.03–0.5%	0.2%	0.06–1.5%	0.5%

n.d.: Has not been detected.

**Table 2.** Comparison of the saccharides in this study with those reported in the literatures (ng/m<sup>3</sup>).

Sampling Sites	Site Type	Sampling Time	Particle Type	Concentration Range (ng/m <sup>3</sup> )	Reference
MS, Bologna, Italy	Urban	June 2012–May 2013	PM <sub>2.5</sub>	6.2 (0.6–16.4)	[32]
San Pietro Capofiume, Italy	Rural	June 2012–May 2013	PM <sub>2.5</sub>	38.8 (0.9–200.4)	
Rajim, India	Rural	October–November	PM <sub>2.5</sub>	10166 (4781.1–17979)	[33]
Pingtung, Taiwan	Remote coastal environment (140 m from the seashore)	February–April 2013	PM <sub>2.5</sub>	589.5	[17]
Tsinghua University, Beijing	Urban	November 2010–October 2011	PM <sub>2.5</sub>	600.0 (66.1–389.1)	[34]
Fudan, Shanghai	urban	March 2013–January 2014	PM <sub>2.5</sub>	346.9 (9.4–1652.9)	This study

For the sake of convenience, anhydrosaccharides were defined as the total burning for their burning sources, while monosaccharides and saccharide alcohols were defined as the total biological for their biological sources. Saccharides from the total burning (average annual concentration: 228.0 ng/m<sup>3</sup>) and total biological (average annual concentration: 118.9 ng/m<sup>3</sup>) contributed 65.7% and 34.3% to the total saccharides, respectively.

### 3.1.1. Anhydrosaccharides

Anhydrosaccharides were the most abundant species of saccharides, among which the annual mean value of levoglucosan reached  $180.7 \text{ ng/m}^3$  and contributed 52.1% to the total saccharides. However, also being one of the anhydrosaccharides, mannosan was relatively low, and its annual mean value was only  $48.8 \text{ ng/m}^3$ , accounting for 14.1% of the total saccharides (Figure 2).

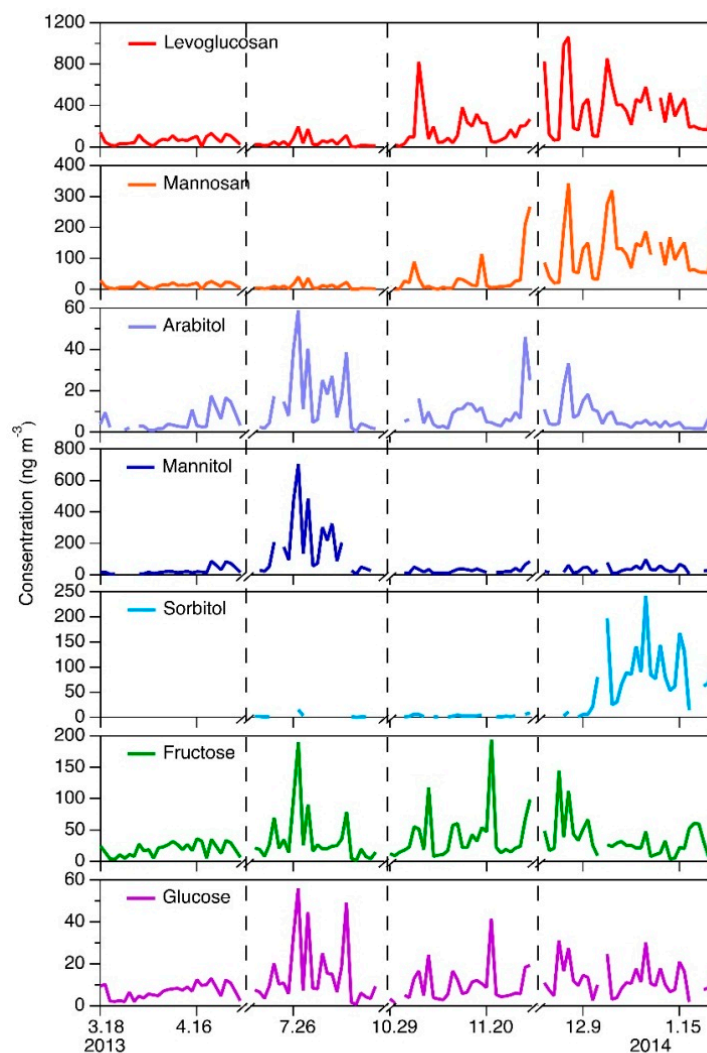


**Figure 2.** Daily concentrations of seven saccharides in  $\text{PM}_{2.5}$  (The areas separated by dotted lines indicate the four seasons of spring, summer, autumn, and winter).

Similar to previous studies, the anhydrosaccharides exhibited pronounced seasonal variations in Shanghai, with high concentrations in cold seasons and low concentrations in warm seasons, as shown in Figure 3. The contribution of the anhydrosaccharides in autumn and winter was 62.7% and 70.4%, and decreased to 46.8% and 18.7% in spring and summer, respectively. High levels of anhydrosaccharides in autumn and winter were in accordance with the fact that open-burning of biomass waste occurs during the harvest season and the heating demand in cold periods. The mean concentration of levoglucosan reached  $392.2 \text{ ng/m}^3$  in winter, which was almost a magnitude higher than that in summer and spring. The significantly high level of levoglucosan in winter and autumn revealed the impact of biomass burning emissions on urban air quality. Except for the heating demand, open burning of crop residues during the post-harvest months (October–November) was still frequently conducted despite its prohibition by the government, resulting in high concentrations of levoglucosan

in the ambient atmosphere [35,36]. Mannosan, the isomer of levoglucosan, was relatively low when compared to levoglucosan, with  $126.5 \text{ ng/m}^3$  in winter and  $9.2 \text{ ng/m}^3$  in summer. The correlation coefficient between the two anhydrosaccharides reached 0.73, indicating similar combustion sources. According to a previous report, levoglucosan and mannosan originate from different types of biomass: Levoglucosan comes from the thermal decomposition of cellulose, usually in hard woods (angiosperm), while mannosan comes from the thermal decomposition of hemicellulose [37], which occurs mainly in soft woods (gymnosperm), and the ratio of levoglucosan/mannosan (L/M) can be used to identify sources of biomass materials.

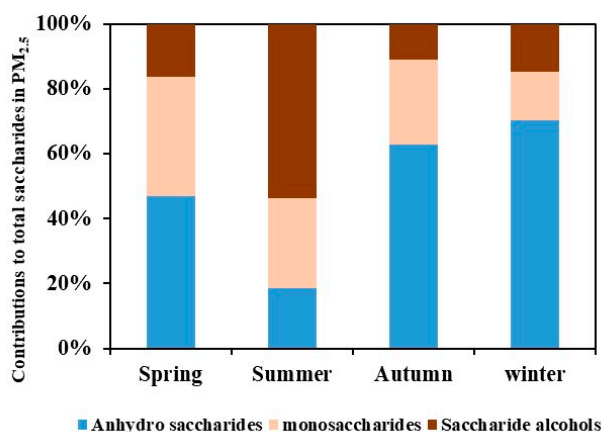


**Figure 3.** Contributions of the three typical saccharides in PM<sub>2.5</sub>.

Previous studies have demonstrated that the L/M ratios from hardwood burning had a range of 15–25, while those of softwood were between 3–10 [38–40]. In general, high values of L/M represented the involvement of more hardwood biomass being burned. L/M ratios of 40–42 were found in the smoke aerosols collected from burning rice straw in a chamber [41], and 40–46 were obtained from the open field burning of wheat straw in the North China Plain [16].

L/M values in this study were relatively low, with 7.26 in winter and 11.29 in autumn; higher values of L/M in autumn than in winter revealed an increase in hardwood burning, which was because of the opening burning of rice straw, a typical species of hard-wood, was conducted during the harvest season of September to November in China.

Recent studies have raised doubts about the stability of levoglucosan during long range transport [42] as levoglucosan can react with free radicals in the atmosphere. Hoffmann et al. found levoglucosan could be resolved in the presence of strong oxidizers [43]. After determining the seasonal variations of levoglucosan over the Northwest Pacific and comparing the results to the model prediction, Mochida et al. found that the measured data were significantly lower than the concentration predicted by the model. This result might be attributed to the oxidative decomposition of levoglucosan through its reaction with OH radicals [44]. During the period of this study, the radiation in spring and summer was obviously higher than that in autumn and winter (Figure 4), and the concentration of levoglucosan had a significantly negative correlation with ozone (Figure S1), indicating that the decrease of levoglucosan was likely attributed to its degradation under a strong oxidizing environment in spring and summer. Therefore, the contribution of biomass burning in summer might be underestimated if levoglucosan is used as the tracer.

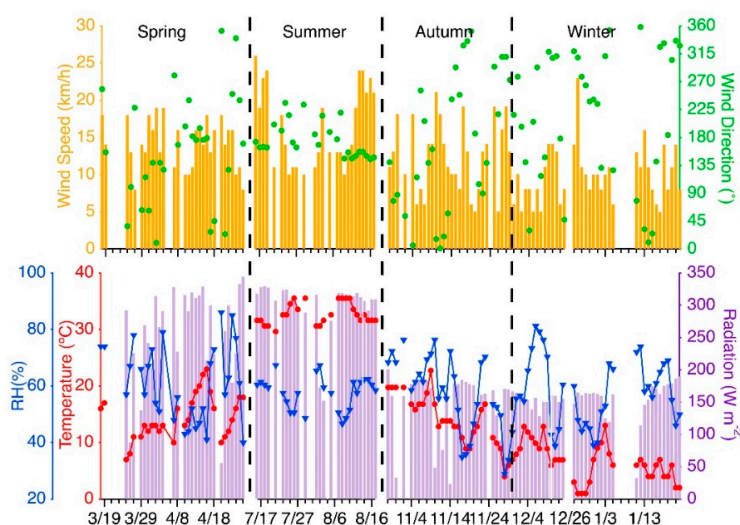


Figure 4. Meteorological conditions of Shanghai in 2013.

### 3.1.2. Saccharide Alcohol

Saccharide alcohols were also important parts of the saccharides. Mannitol, sorbitol, and arabitol contributed 15.1%, 9.2%, and 2.3% to the total saccharides, and the annual mean value of the three species was  $58.9 \text{ ng/m}^3$ ,  $35.7 \text{ ng/m}^3$ , and  $8.7 \text{ ng/m}^3$ , respectively. In contrast to the highest level of anhydrosaccharides in winter, saccharide alcohols contributed the largest proportion in summer, reaching 53.6% of the total saccharides, whereas it was 16.3% and 14.5% in spring and autumn, but only 11.0% in winter (Figure 3). The mean concentration of mannitol in summer ( $172.7 \text{ ng/m}^3$ ) was much higher than that in winter ( $36.8 \text{ ng/m}^3$ ), and a similar pattern also appeared for arabitol, with  $14.9 \text{ ng/m}^3$  in summer and  $7.3 \text{ ng/m}^3$  in winter. Saccharide alcohols are mainly produced by fungal spores and some synergistic effects of photosynthesis, which usually show high activities in the case of high temperatures and adequate light. Moreover, research has shown that mannitol is the product of plant resistance [45], for example, extreme high temperatures cause a water deficit, and mannitol is produced to regulate the osmotic pressure of the cells and to detect and respond to the environment [46]. In Shanghai, the mean temperature in summer was  $33.2 \text{ }^\circ\text{C}$ , while it was only  $6.69 \text{ }^\circ\text{C}$  in winter, and the solar radiation intensity was  $257.2 \text{ W/m}^2$  and  $303.7 \text{ W/m}^2$  in spring and summer, respectively, which was much higher than the  $151.6 \text{ W/m}^2$  in autumn and  $154.6 \text{ W/m}^2$  in winter (Figure 4). The significantly high concentrations of saccharide alcohols during summer suggested that the emissions of saccharide alcohols from biological sources was restrained by meteorological conditions, such as temperature, rainfall, and illumination intensity.

Unlike mannitol and arabitol, sorbitol showed a different seasonal variation, with the highest concentration occurring in winter. Two possible reasons were considered. Firstly, sorbitol is more likely to exist in coarse particles, where Peng et al. found that sorbitol was mainly distributed in sizes of  $3.2\text{--}5.6 \text{ }\mu\text{M}$  in spring and summer, and  $1.8 \text{ }\mu\text{M}$  in winter [23]. Therefore, sorbitol mostly existed in coarse particles in spring, summer, and autumn. However, only fine particles were collected in this study. Therefore, the high concentration of sorbitol in winter could be better understood. On the other hand, the sources of the high concentration of sorbitol in winter obtained in this study needs further discussion.

### 3.1.3. Monosaccharides

The monosaccharides included fructose and glucose, of which the annual mean values were  $32.1 \text{ ng/m}^3$  and  $10.9 \text{ ng/m}^3$  and contributed 8.2% and 2.8% to the total saccharides, respectively (Figure 2). Monosaccharides exhibited similar seasonal variations to the saccharide alcohols,

but showed less fluctuation, with the highest level of 37.0% being in spring, and the contribution in summer and autumn was comparable at 27.7% and 26.3%, respectively, while it was only 15% in winter (Figure 3).

Glucose generally exists in plants in a free form [47], and the activities of soil microorganisms and plant growth will increase the amount of glucose in spring and summer. Soil re-suspension due to high wind speed and farmland cultivation can impel the emission of glucose into the atmosphere. Moreover, the maturing process of crops in autumn may also increase the glucose concentration. However, the emission of glucose is reduced due to the low temperatures in winter, which results in the reduction of plant growth and biological activities.

Fructose is abundantly present in fruit juice and the metabolism of soil microorganism. Fructose has a similar seasonal variation with glucose, and the sum of monosaccharides contributed 37% in spring, 27.7% and 26.3% in summer and autumn, and 15% in winter (Figure 3).

Unlike the significant seasonal variation of the anhydrosaccharides and saccharide alcohols, fructose and glucose in the atmosphere were relatively stable, and can be most likely attributed to being affected by human activities and natural conditions.

### 3.2. PMF Analysis and PSCF Analysis

Positive matrix factorization (PMF) analysis and potential source contribution function analysis (PSCF) provided further investigation of the sources and characterizations of the atmospheric saccharides.

In the PMF analysis, each PMF performance was calculated 30 times with three to seven factors. Concentrations of the seven determined species for the total 150 PM<sub>2.5</sub> samples were subjected for PMF analysis. Four factors were finally resolved (Figure 5), with the F peak value set at zero (the base run result, no extra handling for the weak, and bad species). The error fraction in this study was 10% to estimate the uncertainty, and the extra modeling uncertainty for PMF was 5%.

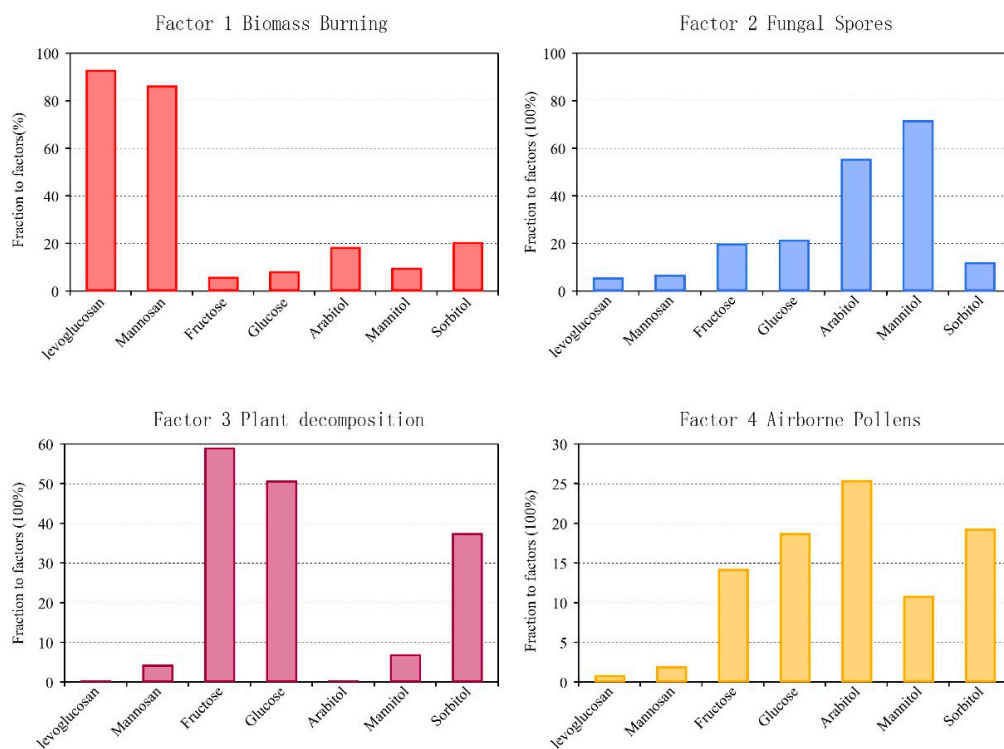


Figure 5. Positive matrix factorization (PMF) factor analysis of saccharides in Shanghai in 2013.

The four factors contributed 46%, 22%, 22%, and 10% to the atmospheric saccharides in Shanghai, respectively. Factor 1 was identified by high levels of levoglucosan (93.2%) and mannosan (86.5%), suggesting the obvious source of biomass burning from crop residues or other biofuels in the local rural areas around Shanghai or other regional input. Factor 2 was dominated by saccharide alcohols (72.0% mannitol and 55.8% arabitol), indicating the sources as fungal spores. As mentioned previously, saccharide alcohols are mainly produced by fungi [48], where mannitol can account for up to 50% of fungal mycelium [10], and spores are necessary for fungal reproduction and survival when entering the breeding stage, which are often released by active processes related to osmotic pressure and surface-tension catapults [49]. Factor 3 was characterized by fructose (59.2%) and glucose (50.9%), indicating the source of plant decomposition. Being abundant in vascular plants, the released fructose and glucose could be attributed to the diagenetic degradation caused by heterotrophic microorganisms in the soil [6]. Soil containing fructose and glucose could be blown up into the atmosphere from dormant or arid land, and agricultural activities could intensify this release, such as tilling in post-harvesting seasons [9]. Factor 4 was dominated by airborne pollen because the amounts of fructose (14.3%), glucose (18.8%), arabitol (25.5%), mannitol (10.9%), and sorbitol (19.4%) were relatively average. Pollen is the reproductive unit of plants and contains these saccharides and saccharide alcohols as nutritional components [50].

As discussed above, the saccharides in PM<sub>2.5</sub> samples in Shanghai came from biomass burning, plant decomposition, pollen, and fungal spores, of which the potential sources were identified by the potential source contribution function (PSCF), as shown below.

As shown in Figure 6, besides local emissions, the potential source areas of saccharide in Shanghai also included the transmission from other regions, such as the Jiangsu, Zhejiang, Jiangxi, and Shandong provinces, and the East China Sea was also identified as a possible source.

Biomass burning sources were mainly distributed in local Shanghai, southern Jiangsu, and northern Zhejiang, and the intensive biomass burning activities in these regions had frequently adversely affected Shanghai's air quality.

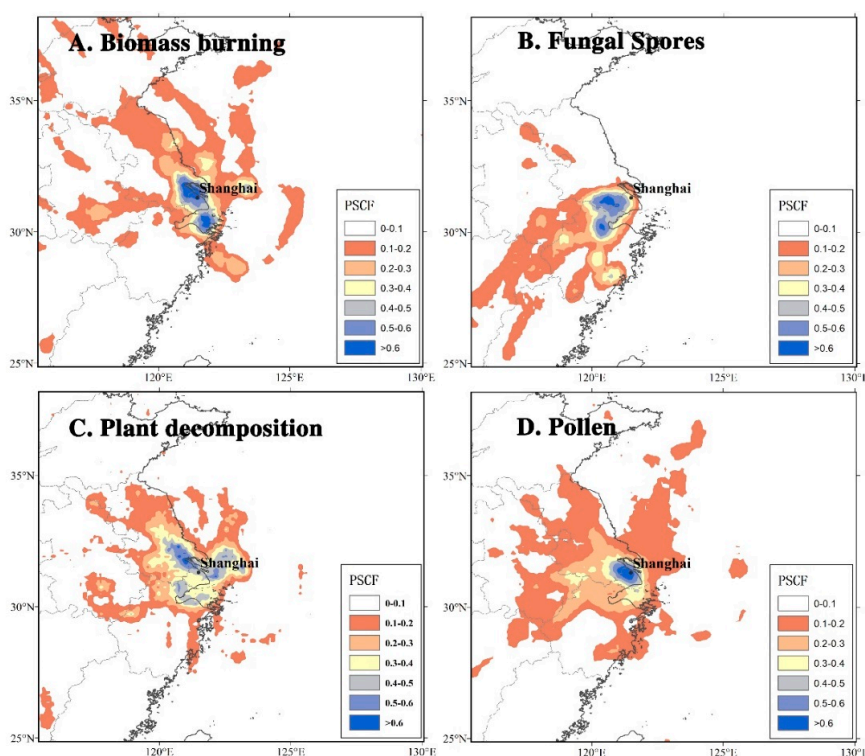


**Figure 6.** Potential source regions for the source of saccharides in Shanghai: (A) Biomass burning; (B) fungal spores; (C) plant decomposition; and (D) pollen.

The formation and distribution of fungal spores depends on the climate, soil, and cultivation system, etc. [51]. Fungal spores are more likely to multiply and diffuse in places with high humidity and temperature. *PSCF* analysis showed that the source of fungal spores was in the regions south of Shanghai, which were characterized with plentiful rainfall and adequate vegetation coverage.

The high *PSCF* values of plant decomposition were distributed in YRD (Yangtze River Delta), because saccharides produced by the decomposition of plants in continental areas could be sprayed into the atmosphere through soil suspension. However, high *PSCF* values of plant decomposition were also found in the East China Sea. Saccharides have been reported to account for as much as 63% of total water-soluble organic components in oceanic aerosols [6]. The oceanic source of saccharides is likely due to the decomposition of lower plants, such as algae and lichens, in the sea water, which needs further biological research.

Pollen grains are usually coarse with various shapes and hard shells, which results in the relatively short retention time in the atmosphere. Therefore, the potential source regions of pollen were mostly concentrated locally to Shanghai.

### 3.3. The Formation Process of High Level of Levoglucosan

A process of levoglucosan with significant fluctuation was detected, of which the concentration reached 285.7 ng/m<sup>3</sup> from 4 November to 9 November, which was much higher than the mean value of 165.7 ng/m<sup>3</sup> in autumn. The average L/M value of the period was 26.5 and, in particular, for the 7 November and 9 November, the L/M values were 64.8 and 56.7, a little higher than the ratios of 40–42 from burning rice straw in a chamber [41] and the open field burning of wheat straw [16]. Therefore, the sudden increase in saccharides was due to the treatment of the crop waste by open burning directly in the field.

The backward trajectories and the distribution of fire spots during the period were shown in Figure 7, which indicated that the air mass was transported through the areas of intensive fire spots. From 4 November, the number of fire spots increased gradually, the air mass came from the northeastern part of China on 4 November and 5 November, and the concentration of levoglucosan on the two days was 96.3 ng/m<sup>3</sup> and 96.9 ng/m<sup>3</sup>, respectively. The fire spots reached a maximum on 6 November and 7 November (Figure 7), when the concentration of levoglucosan was the highest on those two days. The results indicated that the concentration of levoglucosan was consistent with the variations in fire spot intensity. Specifically, as can be seen in Figure 7, the number of fire spots sharply increased on 6 November when the air mass trajectory hovered in Shanghai, indicating unfavorable climate conditions. Therefore, the concentration of levoglucosan reached the highest value of 823.6 ng/m<sup>3</sup>. On 7 November, the trajectory was from western parts of Shanghai, such as Anhui and Henan, and the meteorological conditions were beneficial to the expansion of air mass, which resulted in the obvious decrease of levoglucosan compared to 6 November, but still a high value of 425.9 ng/m<sup>3</sup>. The meteorological conditions significantly improved from 8 November, and the concentration of levoglucosan decreased to 78.3 ng/m<sup>3</sup> on 8 November, but increased to 195.3 ng/m<sup>3</sup> again on 9 November when the trajectory was from southwestern parts of Shanghai, such as Zhejiang and Jiangxi, where intensive fire spots are distributed. Therefore, it can be concluded that, in addition to the local pollution, the concentration of levoglucosan in Shanghai was mainly influenced by the transport of biomass burning emissions from the southwestern areas.

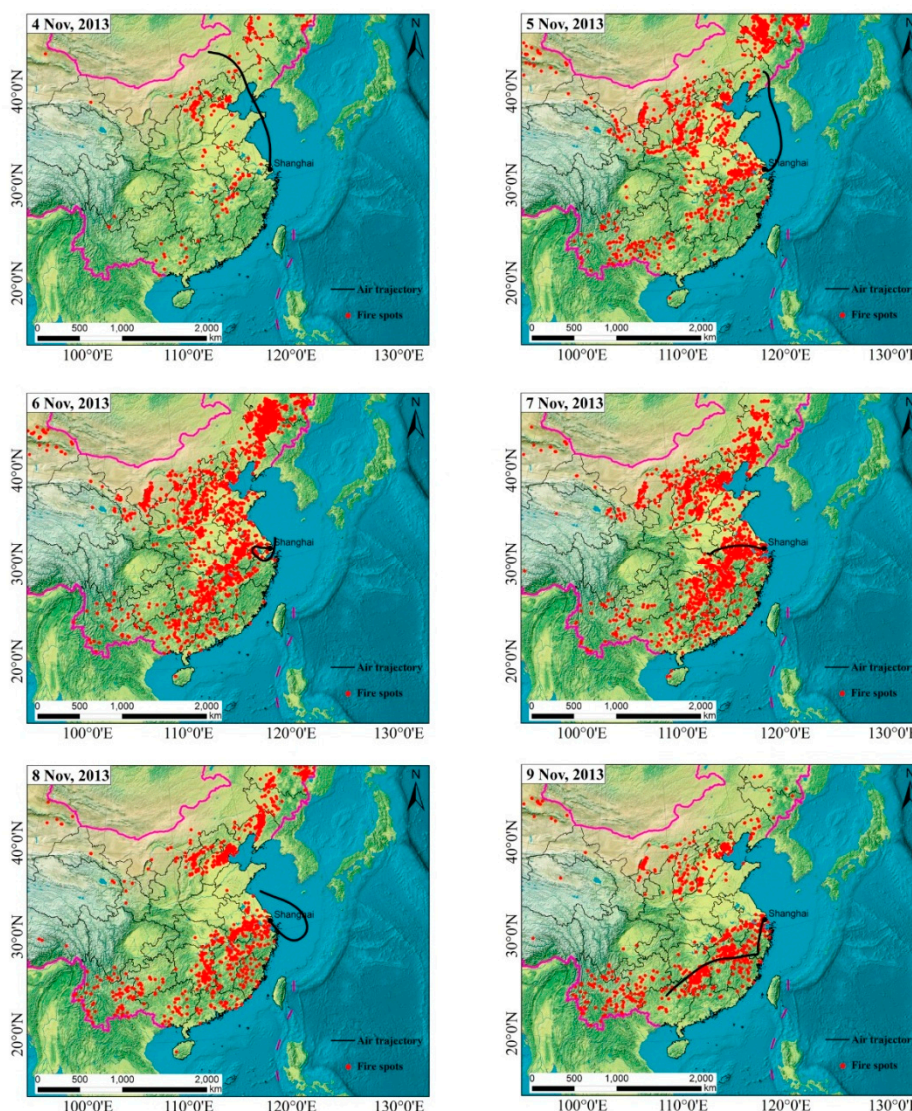


**Figure 7.** Fire spots’ distribution combined with the 48-h backward trajectory analysis during the period.

### 3.4. Relations between Saccharides and PM<sub>2.5</sub> Levels

Over the past few decades, China has suffered serious air pollution [52,53], especially in the most developed and highly populated regions, such as the YRD, Pearl River Delta (PRD), and Beijing-Tianjin-Hebei (BTH) [54]. Severe air pollution of a long duration covering a wide area across China occurred in December 2013, which provided a chance to track the variation of aerosol particles and their constituents. During this pollution period, hourly maximum concentrations of PM<sub>2.5</sub> in Shanghai exceeded 600 µg/m<sup>3</sup>. Many studies have focused on the chemical components and temporal variation of inorganic ions and elements during the haze particles [55,56]. However, little information related to saccharides was available during the pollution period [57]. The compositions of the saccharide alcohols showed opposite trends when compared to the particulate matters. During the period when the averaged concentration of PM<sub>2.5</sub> was above 150 µg/m<sup>3</sup> (named pollution period), the concentrations of arabitol, mannitol, and sorbitol were 3.78 ng/m<sup>3</sup>, 29.07 ng/m<sup>3</sup>, and 44.16 ng/m<sup>3</sup>, respectively, but increased to 8.9 ng/m<sup>3</sup>, 44.8 ng/m<sup>3</sup>, and 112.1 ng/m<sup>3</sup> when the concentration of PM<sub>2.5</sub> was lower than 100 µg/m<sup>3</sup> (named clear period). The obvious reduction in saccharide alcohols during the heavy PM<sub>2.5</sub> pollution period suggested an inverse influence of haze pollution on biological

activities, which might further result in the reduction of agricultural production. Some studies have found that the average level of microbial activity was  $100.33 \text{ ng/m}^3$  of sodium fluorescein on sunny days, which decreased to  $56.53 \text{ ng/m}^3$  of sodium fluorescein on hazy days. When the haze was mixed with fog for several days the microbial activity reduced to 37.7% of the level of sunny days [58]. Studies have also found that haze may damage the hierarchy and functions of the ecosystem, leading to the loss of crops, which may reduce biodiversity and even damage the biological chain. The reduction of biological activity was demonstrated from the perspective of saccharides in this study.

Fructose showed a similar trend as  $\text{PM}_{2.5}$  did, with  $35.7 \text{ ng/m}^3$  during the pollution period and  $13.5 \text{ ng/m}^3$  in the clear period. In contrast, the concentration of glucose was very close in the two periods. Having originated from soil suspension, the concentrations of fructose and glucose should increase in the atmosphere, with an increase of wind speed. However, the mean wind speed was comparable in the two periods, suggesting there likely exists another reason for the difference.

The concentrations of levoglucosan in the two periods were  $379.1 \text{ ng/m}^3$  and  $414.3 \text{ ng/m}^3$ . Similarly, mannosan was  $133.3 \text{ ng/m}^3$  and  $146.7 \text{ ng/m}^3$  for the two periods, respectively. Anhydrosaccharides showed no obvious difference, suggesting that biomass burning was not the trigger factor for the heavy air pollution in the winter of 2013 in China. Secondary inorganic components (sulfate, nitrate, and ammonium), together with the unfavorable meteorological conditions, have been reported to be responsible for the heavy pollution processes [59,60].

#### 4. Conclusions

In this study,  $\text{PM}_{2.5}$  samples were collected to identify the composition, source, and seasonal variations of the atmospheric saccharides, and the characteristics of saccharides under different levels of pollution were also discussed. The concentration of the total saccharides had a range of  $9.4 \text{ ng/m}^3$  to  $1652.9 \text{ ng/m}^3$  (average  $346.9 \text{ ng/m}^3$ ) during the whole year, with high concentrations of anhydrosaccharides from burning sources in the cold season and high concentrations of saccharide alcohols from biological sources during the warm seasons. Four factors of biomass burning, fungal spores, plant decomposition, and airborne pollens were obtained through PMF analysis, with contributions of 46%, 22%, 22%, and 10% of the atmospheric saccharides in Shanghai. The results of the PSCF analysis of the sources indicated that, besides local emissions, the potential source areas of saccharides in Shanghai also included transmission from other regions, such as the Jiangsu, Zhejiang, Jiangxi, and Shandong provinces, and the East China Sea was also identified as a possible source. The resolution of the backward trajectory and fire points showed the process of high concentrations of levoglucosan due to biomass burnings. Concentrations of anhydrosaccharides were relatively stable under clear conditions and during the pollution period, while saccharide alcohols exhibited an obvious variation, indicating that biomass burning was not the core reason for the haze pollution. However, haze air pollution could lead to a significant reduction in biomass activity from the perspective of the saccharide alcohols.

**Supplementary Materials:** The following are available online at <http://www.mdpi.com/2073-4433/9/7/274/s1>, Figure S1: The negative correlation between levoglucosan ( $\text{ng/m}^3$ ) and  $\text{O}_3$  ( $\mu\text{g/m}^3$ ), Table S1: List of days under different pollution levels: heavy haze ( $>150 \mu\text{g/m}^3$ , 17 days); clear ( $<100 \mu\text{g/m}^3$ , 8 days).

**Author Contributions:** M.X. conducted the experiments and wrote this paper; Q.W. made suggestions for this paper; X.Q. and G.Y. conducted the sampling activities; C.D. reviewed the general idea in this paper. All authors have approved the final manuscript.

**Funding:** This research was funded by National Key Research and Development Program of China (Grant number 2016YFA0601304) and the National Natural Science Foundation of China (Grant number 21777029).

**Conflicts of Interest:** The authors declare no conflict of interest.

#### References

1. Herrmann, H.; Ervens, B.; Jacobi, H.W.; Wolke, R.; Nowacki, P.; Zellner, R. CAPRAM2.3: A chemical aqueous phase radical mechanism for tropospheric chemistry. *J. Atmos. Chem.* **2000**, *36*, 231–284. [[CrossRef](#)]

2. Duarte, R.M.B.O.; Santos, E.B.H.; Pio, C.A.; Duarte, A.C. Comparison of structural features of water-soluble organic matter from atmospheric aerosols with those of aquatic humic substances. *Atmos. Environ.* **2007**, *41*, 8100–8113. [[CrossRef](#)]
3. Lopes, S.P.; Matos, J.T.V.; Silva, A.M.S.; Duarte, A.C.; Duarte, R.M.B.O. <sup>1</sup>H NMR studies of water- and alkaline-soluble organic matter from fine urban atmospheric aerosols. *Atmos. Environ.* **2015**, *119*, 374–380. [[CrossRef](#)]
4. Fuzzi, S.; Decesari, S.; Facchini, M.C.; Cavalli, F.; Emblico, L.; Mircea, M.; Andreae, M.O.; Trebs, I.; Hoffer, A.; Guyon, P.; et al. Overview of the inorganic and organic composition of size-segregated aerosol in Rondonia, Brazil, from the biomass-burning period to the onset of the wet season. *J. Geophys. Res. Atmos.* **2007**, *112*. [[CrossRef](#)]
5. Wang, G.; Chen, C.; Li, J.; Zhou, B.; Xie, M.; Hu, S.; Kawamura, K.; Chen, Y. Molecular composition and size distribution of sugars, sugar-alcohols and carboxylic acids in airborne particles during a severe urban haze event caused by wheat straw burning. *Atmos. Environ.* **2011**, *45*, 2473–2479. [[CrossRef](#)]
6. Simoneit, B.R.T.; Elias, V.O.; Kobayashi, M.; Kawamura, K.; Rushdi, A.I.; Medeiros, P.M.; Rogge, W.F.; Didyk, B.M. Sugars—Dominant water-soluble organic compounds in soils and characterization as tracers in atmospheric particulate matter. *Environ. Sci. Technol.* **2004**, *38*, 5939–5949. [[CrossRef](#)] [[PubMed](#)]
7. Yan, C.Q.; Zheng, M.; Sullivan, A.P.; Bosch, C.; Desyaterik, Y.; Andersson, A.; Li, X.Y.; Guo, X.S.; Zhou, T.; Gustafsson, O.; et al. Chemical characteristics and light-absorbing property of water-soluble organic carbon in Beijing: Biomass burning contributions. *Atmos. Environ.* **2015**, *121*, 4–12. [[CrossRef](#)]
8. Despres, V.R.; Huffman, J.A.; Burrows, S.M.; Hoose, C.; Safatov, A.S.; Buryak, G.; Froehlich-Nowoisky, J.; Elbert, W.; Andreae, M.O.; Poeschl, U.; et al. Primary biological aerosol particles in the atmosphere: A review. *Tellus Ser. B Chem. Phys. Meteorol.* **2012**, *64*. [[CrossRef](#)]
9. Rogge, W.F.; Medeiros, P.M.; Simoneit, B.R.T. Organic marker compounds in surface soils of crop fields from the San Joaquin Valley fugitive dust characterization study. *Atmos. Environ.* **2007**, *41*, 8183–8204. [[CrossRef](#)]
10. Véléz, H.; Glassbrook, N.J.; Daub, M.E. Mannitol metabolism in the phytopathogenic fungus *Alternaria alternata*. *Fungal Genet. Biol.* **2007**, *44*, 258–268. [[CrossRef](#)] [[PubMed](#)]
11. Fabbri, D.; Torri, C.; Simonei, B.R.T.; Marynowski, L.; Rushdi, A.I.; Fabianska, M.J. Levoglucosan and other cellulose and lignin markers in emissions from burning of Miocene lignites. *Atmos. Environ.* **2009**, *43*, 2286–2295. [[CrossRef](#)]
12. Fraser, M.P.; Lakshmanan, K. Using levoglucosan as a molecular marker for the long-range transport of biomass combustion aerosols. *Environ. Sci. Technol.* **2000**, *34*, 4560–4564. [[CrossRef](#)]
13. Jung, J.; Lee, S.; Kim, H.; Kim, D.; Lee, H.; Oh, S. Quantitative determination of the biomass-burning contribution to atmospheric carbonaceous aerosols in Daejeon, Korea, during the rice-harvest period. *Atmos. Environ.* **2014**, *89*, 642–650. [[CrossRef](#)]
14. Zhang, Y.-N.; Zhang, Z.-S.; Chan, C.-Y.; Engling, G.; Sang, X.-F.; Shi, S.; Wang, X.-M. Levoglucosan and carbonaceous species in the background aerosol of coastal southeast China: Case study on transport of biomass burning smoke from the Philippines. *Environ. Sci. Pollut. Res.* **2012**, *19*, 244–255. [[CrossRef](#)] [[PubMed](#)]
15. Bond, T.C.; Streets, D.G.; Yarber, K.F.; Nelson, S.M.; Woo, J.H.; Klimont, Z. A technology-based global inventory of black and organic carbon emissions from combustion. *J. Geophys. Res. Atmos.* **2004**, *109*. [[CrossRef](#)]
16. Fu, P.; Kawamura, K.; Kobayashi, M.; Simoneit, B.R.T. Seasonal variations of sugars in atmospheric particulate matter from Gosan, Jeju Island: Significant contributions of airborne pollen and Asian dust in spring. *Atmos. Environ.* **2012**, *55*, 234–239. [[CrossRef](#)]
17. Tsai, Y.I.; Sopajaree, K.; Kuo, S.C.; Hsin, T.Y. Chemical Composition and Size-Fractionated Origins of Aerosols over a Remote Coastal Site in Southern Taiwan. *Aerosol Air Qual. Res.* **2015**, *15*, 2549–2570. [[CrossRef](#)]
18. Tobo, Y.; Prenni, A.J.; DeMott, P.J.; Huffman, J.A.; McCluskey, C.S.; Tian, G.; Pöhlker, C.; Poeschl, U.; Kreidenweis, S.M. Biological aerosol particles as a key determinant of ice nuclei populations in a forest ecosystem. *J. Geophys. Res. Atmos.* **2013**, *118*, 10100–10110. [[CrossRef](#)]
19. Zawadowicz, M.A.; Froyd, K.D.; Murphy, D.M.; Cziczo, D.J. Improved identification of primary biological aerosol particles using single-particle mass spectrometry. *Atmos. Chem. Phys.* **2017**, *17*, 7193–7212. [[CrossRef](#)]

20. Yue, S.; Ren, H.; Fan, S.; Wei, L.; Zhao, J.; Bao, M.; Hou, S.; Zhan, J.; Zhao, W.; Ren, L.; et al. High Abundance of Fluorescent Biological Aerosol Particles in Winter in Beijing, China. *ACS Earth Space Chem.* **2017**, *1*, 493–502. [[CrossRef](#)]
21. Lin, Y.; Huang, K.; Zhuang, G.; Fu, J.S.; Wang, Q.; Liu, T.; Deng, C.; Fu, Q. A multi-year evolution of aerosol chemistry impacting visibility and haze formation over an Eastern Asia megacity, Shanghai. *Atmos. Environ.* **2014**, *92*, 76–86. [[CrossRef](#)]
22. Li, P.; Li, X.; Yang, C.; Wang, X.; Chen, J.; Collett, J.L., Jr. Fog water chemistry in Shanghai. *Atmos. Environ.* **2011**, *45*, 4034–4041. [[CrossRef](#)]
23. Peng, J.; Li, M.; Zhang, P.; Gong, S.; Zhong, M.; Wu, M.; Zheng, M.; Chen, C.; Wang, H.; Lou, S. Investigation of the sources and seasonal variations of secondary organic aerosols in PM<sub>2.5</sub> in Shanghai with organic tracers. *Atmos. Environ.* **2013**, *79*, 614–622.
24. Ashbaugh, L.L.; Malm, W.C.; Sadeh, W.Z. A Residence Time Probability Analysis of Sulfur Concentrations at Grand-Canyon-National-Park. *Atmos. Environ.* **1985**, *19*, 1263–1270. [[CrossRef](#)]
25. Wang, Y.Q.; Zhang, X.Y.; Draxler, R.R. TrajStat: GIS-based software that uses various trajectory statistical analysis methods to identify potential sources from long-term air pollution measurement data. *Environ. Model. Softw.* **2009**, *24*, 938–939. [[CrossRef](#)]
26. Cheng, M.D.; Hopke, P.K.; Barrie, L.; Rippe, A.; Olson, M.; Landsberger, S. Qualitative determination of source regions of aerosol in canadian high arctic. *Environ. Sci. Technol.* **1993**, *27*, 2063–2071. [[CrossRef](#)]
27. Hopke, P.K.; Barrie, L.A.; Li, S.M.; Cheng, M.D.; Li, C.; Xie, Y. Possible sources and preferred pathways for biogenic and non-sea-salt sulfur for the high arctic. *J. Geophys. Res. Atmos.* **1995**, *100*, 16595–16603. [[CrossRef](#)]
28. Polissar, A.V.; Hopke, P.K.; Paatero, P.; Kaufmann, Y.J.; Hall, D.K.; Bodhaine, B.A.; Dutton, E.G.; Harris, J.M. The aerosol at Barrow, Alaska: Long-term trends and source locations. *Atmos. Environ.* **1999**, *33*, 2441–2458. [[CrossRef](#)]
29. Xu, X.; Akhtar, U.S. Identification of potential regional sources of atmospheric total gaseous mercury in Windsor, Ontario, Canada using hybrid receptor modeling. *Atmos. Chem. Phys.* **2010**, *10*, 7073–7083. [[CrossRef](#)]
30. Paatero, P. Least squares formulation of robust non-negative factor analysis. *Chemom. Intell. Lab. Syst.* **1997**, *37*, 23–35. [[CrossRef](#)]
31. Paatero, P.; Hopke, P.K. Rotational tools for factor analytic models. *J. Chemom.* **2010**, *23*, 91–100. [[CrossRef](#)]
32. Pietrogrande, M.C.; Bacco, D.; Visentin, M.; Ferrari, S.; Casali, P. Polar organic marker compounds in atmospheric aerosol in the Po Valley during the Supersito campaigns—Part 2: Seasonal variations of sugars. *Atmos. Environ.* **2014**, *97*, 215–225. [[CrossRef](#)]
33. Nirmalkar, J.; Deshmukh, D.K.; Deb, M.K.; Tsai, Y.I.; Sopajaree, K. Mass loading and episodic variation of molecular markers in PM<sub>2.5</sub> aerosols over a rural area in eastern central India. *Atmos. Environ.* **2015**, *117*, 41–50. [[CrossRef](#)]
34. Liang, L.; Engling, G.; Du, Z.; Cheng, Y.; Duan, F.; Liu, X.; He, K. Seasonal variations and source estimation of saccharides in atmospheric particulate matter in Beijing, China. *Chemosphere* **2016**, *150*, 365–377. [[CrossRef](#)] [[PubMed](#)]
35. Yan, X.Y.; Ohara, T.; Akimoto, H. Bottom-up estimate of biomass burning in mainland China. *Atmos. Environ.* **2006**, *40*, 5262–5273. [[CrossRef](#)]
36. Li, X.; Chen, M.X.; Le, H.P.; Wang, F.W.; Guo, Z.G.; Iinuma, Y.; Chen, J.M.; Herrmann, H. Atmospheric outflow of PM<sub>2.5</sub> saccharides from megacity Shanghai to East China Sea: Impact of biological and biomass burning sources. *Atmos. Environ.* **2016**, *143*, 1–14. [[CrossRef](#)]
37. Simoneit, B.R.T. Biomass burning—A review of organic tracers for smoke from incomplete combustion. *Appl. Geochem.* **2002**, *17*, 129–162. [[CrossRef](#)]
38. Schmid, C.; Marr, L.L.; Caseiro, A.; Kotianova, P.; Berner, A.; Bauer, H.; Kasper-Giebl, A.; Puxbaum, H. Chemical characterisation of fine particle emissions from wood stove combustion of common woods growing in mid-European Alpine regions. *Atmos. Environ.* **2008**, *42*, 126–141. [[CrossRef](#)]
39. Verma, S.K.; Kawamura, K.; Chen, J.; Fu, P.; Zhu, C. Thirteen years of observations on biomass burning organic tracers over Chichijima Island in the western North Pacific: An outflow region of Asian aerosols. *J. Geophys. Res. Atmos.* **2015**, *120*, 4155–4168. [[CrossRef](#)]

40. Fu, P.; Zhuang, G.; Sun, Y.; Wang, Q.; Chen, J.; Ren, L.; Yang, F.; Wang, Z.; Pan, X.; Li, X.; et al. Molecular markers of biomass burning, fungal spores and biogenic SOA in the Taklimakan desert aerosols. *Atmos. Environ.* **2016**, *130*, 64–73. [[CrossRef](#)]
41. Engling, G.; Lee, J.J.; Tsai, Y.W.; Lung, S.C.C.; Chou, C.C.K.; Chan, C.Y. Size-Resolved Anhydrosugar Composition in Smoke Aerosol from Controlled Field Burning of Rice Straw. *Aerosol Sci. Technol.* **2009**, *43*, 662–672. [[CrossRef](#)]
42. Hennigan, C.J.; Sullivan, A.P.; Collett, J.L., Jr.; Robinson, A.L. Levoglucosan stability in biomass burning particles exposed to hydroxyl radicals. *Geophys. Res. Lett.* **2010**, *37*. [[CrossRef](#)]
43. Hoffmann, D.; Tilgner, A.; Iinuma, Y.; Herrmann, H. Atmospheric Stability of Levoglucosan: A Detailed Laboratory and Modeling Study. *Environ. Sci. Technol.* **2010**, *44*, 694–699. [[CrossRef](#)] [[PubMed](#)]
44. Mochida, M.; Kawamura, K.; Fu, P.; Takemura, T. Seasonal variation of levoglucosan in aerosols over the western North Pacific and its assessment as a biomass-burning tracer. *Atmos. Environ.* **2010**, *44*, 3511–3518. [[CrossRef](#)]
45. Prat, H. Regarding the relations existing between the gradient of resistance to heat, maturation and hydration of plant tissues. *C. R. Hebd. Seances Acad. Sci.* **1944**, *218*, 518–519.
46. Sinha, A.; Gupta, S.R.; Rana, R.S. Effects of osmotic tension and salt stress on germination of 3 grass species. *Plant Soil* **1982**, *69*, 13–19. [[CrossRef](#)]
47. Ma, S.; Wang, Z.; Bi, X.; Sheng, G.; Fu, J. Composition and source of saccharides in aerosols in Guangzhou, China. *Chin. Sci. Bull.* **2009**, *54*, 4500–4506. [[CrossRef](#)]
48. Bauer, H.; Claeys, M.; Vermeylen, R.; Schueller, E.; Weinke, G.; Berger, A.; Puxbaum, H. Arabitol and mannitol as tracers for the quantification of airborne fungal spores. *Atmos. Environ.* **2008**, *42*, 588–593. [[CrossRef](#)]
49. Pringle, A.; Patek, S.N.; Fischer, M.; Stolze, J.; Money, N.P. The captured launch of a ballistospore. *Mycologia* **2005**, *97*, 866–871. [[CrossRef](#)] [[PubMed](#)]
50. Miguel, A.G.; Taylor, P.E.; House, J.; Glovsky, M.M.; Flagan, R.C. Meteorological influences on respirable fragment release from Chinese elm pollen. *Aerosol Sci. Technol.* **2006**, *40*, 690–696. [[CrossRef](#)]
51. Porter, W.M.; Robson, A.D.; Abbott, L.K. Field Survey of the Distribution of Vesicular Arbuscular Mycorrhizal Fungi in Relation to Soil-pH. *J. Appl. Ecol.* **1987**, *24*, 659–662. [[CrossRef](#)]
52. Wang, J.; Hu, Z.M.; Chen, Y.Y.; Chen, Z.L.; Xu, S.Y. Contamination characteristics and possible sources of PM<sub>10</sub> and PM<sub>2.5</sub> in different functional areas of Shanghai, China. *Atmos. Environ.* **2013**, *68*, 221–229. [[CrossRef](#)]
53. Ouyang, Y. China wakes up to the crisis of air pollution. *Lancet Respir. Med.* **2013**, *1*, 12. [[CrossRef](#)]
54. Wang, S.J.; Zhou, C.S.; Wang, Z.B.; Feng, K.S.; Hubacek, K. The characteristics and drivers of fine particulate matter (PM<sub>2.5</sub>) distribution in China. *J. Clean. Prod.* **2017**, *142*, 1800–1809. [[CrossRef](#)]
55. Han, T.; Qiao, L.; Zhou, M.; Qu, Y.; Du, J.; Liu, X.; Lou, S.; Chen, C.; Wang, H.; Zhang, F.; et al. Chemical and optical properties of aerosols and their interrelationship in winter in the megacity Shanghai of China. *J. Environ. Sci.* **2015**, *27*, 59–69. [[CrossRef](#)] [[PubMed](#)]
56. Sun, Y.L.; Zhuang, G.S.; Tang, A.H.; Wang, Y.; An, Z.S. Chemical characteristics of PM<sub>2.5</sub> and PM<sub>10</sub> in haze-fog episodes in Beijing. *Environ. Sci. Technol.* **2006**, *40*, 3148–3155. [[CrossRef](#)] [[PubMed](#)]
57. Li, X.; Jiang, L.; Hoa, L.P.; Lyu, Y.; Xu, T.T.; Yang, X.; Iinuma, Y.; Chen, J.M.; Herrmann, H. Size distribution of particle-phase sugar and nitrophenol tracers during severe urban haze episodes in Shanghai. *Atmos. Environ.* **2016**, *145*, 115–127. [[CrossRef](#)]
58. Zhong, X.; Qi, J.; Li, H.; Dong, L.; Gao, D. Seasonal distribution of microbial activity in bioaerosols in the outdoor environment of the Qingdao coastal region. *Atmos. Environ.* **2016**, *140*, 506–513. [[CrossRef](#)]
59. Behera, S.N.; Cheng, J.; Huang, X.; Zhu, Q.; Liu, P.; Balasubramanian, R. Chemical composition and acidity of size-fractionated inorganic aerosols of 2013–14 winter haze in Shanghai and associated health risk of toxic elements. *Atmos. Environ.* **2015**, *122*, 259–271. [[CrossRef](#)]
60. Li, R.; Yang, X.; Fu, H.; Hu, Q.; Zhang, L.; Chen, J. Characterization of typical metal particles during haze episodes in Shanghai, China. *Chemosphere* **2017**, *181*, 259–269. [[CrossRef](#)] [[PubMed](#)]

